Energy Balance and Structural Regimes of Radiative Shocks in Optically Thick Media

R. Paul Drake

(Invited Paper)

***Abstract*—Radiative shocks in optically thick media are of fundamental interest. They exist in various astrophysical circumstances, and are likely to be explored in future experiments. This paper presents the relevant fluid theory for arbitrary initial conditions. In the approximation that the shock structure has three distinct layers, it uses energy-balance arguments to provide a semiquantitative assessment of key features of these systems and uses an approximate treatment of radiative transfer to obtain the shock structure.**

***Index Terms*—Radiation hydrodynamics, radiative shocks.**

I. Introduction

In any shock wave, heating at the shock transition leads to heating, slowing, and compression of the matter entering the shock from "upstream." If the shock wave is fast enough, the heating becomes so large that radiation from the heated matter carries a significant energy flux back upstream and alters the structure of the shock. At this point, the shock becomes a radiative shock, in which the radiative energy flux and/or pressure plays an essential role in the dynamics. Radiative shocks exist in a wide variety of astrophysical systems and are becoming an area of study in laboratory experiments at high energy density [1]–[9]. In many, although far from all, of the astrophysical systems, such shocks occur in environments from which the radiation readily escapes and in which the radiative energy is carried by line radiation. The theory of such shocks very quickly becomes entangled in the radiative transfer calculations involving such lines. There are many examples of such work, including, for example, papers involving Gillet and collaborators [10]. In contrast, a number of cases of interest exist in regimes where continuum radiation is important, where radiation does not easily escape the system, and where an approach based on spectrally averaged opacities may prove to be productive. These include the laboratory experiments, the current generation of astrophysical radiation-hydrodynamic codes, and some astrophysical environments including some shocks in accretion disks, [11] shocks within stars [12] and shocks produced when active galactic nuclei capture stars [13].

Manuscript received October 1, 2006; revised December 20, 2006. This work was supported by the University of Michigan and by the National Nuclear Security Administration under the Stewardship Science Academic Alliances program through DOE Research Grant DE-FG52-03NA00064 by the National Nuclear Security Agency.

The author is with the Department of Atmospheric, Oceanic, and Space Sciences and the Applied Physics Program, University of Michigan, Ann Arbor, MI 48109 USA (e-mail: rpdrake@umich.edu).

Digital Object Identifier 10.1109/TPS.2007.892142

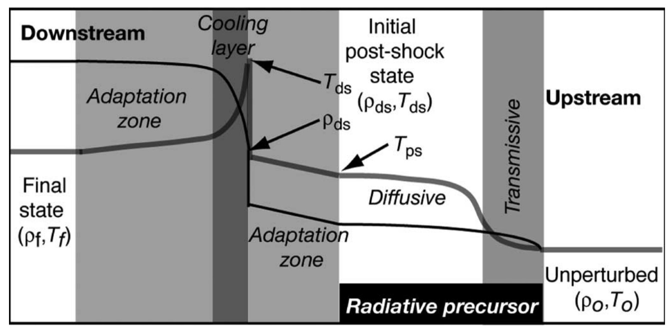

Fig. 1. Schematic depiction of an OTR shock. Directions are chosen such that the shock moves from left to right in the inertial frame of the laboratory.

No matter what the properties of the system are, any shock becomes radiative at high enough velocity. Matter enters the shock from upstream with a speed designated as the "shock velocity" u_s. The incoming matter of density ρ_o carries an energy flux proportional to $\rho_\mathrm{o} u_\mathrm{s}^3$. In the most common case that the radiation pressure p_R remains small compared to the material pressure p, the final postshock temperature T_f is proportional to u_s^2. In this regime, the radiation flux from the heated matter is proportional, through T_f^4, to u_s^8. As a result, the ratio of thermal radiation flux to incoming material energy flux scales as $u_\mathrm{s}^5/\rho_\mathrm{o}$ and rapidly increases with u_s. Even if the optical depth of the shock-heated region is quite small and the incoming matter is hot, above some velocity, the radiative flux will become essential to the behavior of the shock. In the simpler case that the upstream radiation pressure p_R is of order or greater than the material pressure p, then the shock would be described as radiative at any velocity.

Here, we focus on the behavior of radiative shocks within systems that are "optically thick," meaning that the radiation produced by thermal processes in such systems cannot escape the system. We designate such shocks as optically-thick-radiative (OTR) shocks. We will discuss them in a frame of reference called the "shock frame," in which the viscous transition in fluid parameters is at rest. The structure of OTR shocks includes several zones, illustrated schematically in Fig. 1. Moving from upstream to "downstream," there is an unperturbed zone, a radiative precursor, a cooling layer, and a final state. We designate these zones below by subscripts o, p, cl, and f, respectively. The precursor and the final state are both separated from the cooling layer by adaptation zones where the plasma parameters change slowly over distances of several optical depths. These are caused by the influence of the radiation from the cooling layer on the surrounding material. These adaptation zones are not important for the energy balance but they do affect the exact profiles, and they also introduce some potential semantic confusion, as is discussed below. There is a density jump that separates the precursor adaptation zone and the cooling layer, and we designate the properties just upstream or just downstream of this density jump by the subscripts us and ds, respectively. In some literature, the density jump is referred to as the "shock," while in other literature, the entire structure is referred to as the shock. This is further discussed below. In addition, there are regimes either of very weak shocks or of shocks dominated by radiation pressure in which the density does not increase abruptly but rather is smoothed out into a more-gradual transition. These regimes are discussed elsewhere [14], [15] and will not concern us here.

Theoretical work on OTR shocks began in the 1950s, with papers employing semiquantitative arguments to assess their structure and behavior [16]–[22]. This work through the mid-1960s is summarized in the text by Zel'dovich and Razier [23]. The later book by Mihalas and Weibel-Mihalas [14] provides a similar discussion while that by Castor [24] provides an alternative analysis from similar assumptions, reaching similar conclusions. These analyses, consistent with their goals, ignore the adaptation zones. This introduces an ambiguity in the location of the temperature in the precursor at the density jump T_{us} as they can only consider the value of the temperature beyond the adaptation zone. We will label the temperature at the boundary of the adaptation zone as T_{ps}. This in turn introduces a small error in the inferred behavior at the density jump. All of these details are no problem from the point of view of providing an approximate physical analysis. However, they introduce the need for great care in comparing such analyses to more sophisticated treatments, whether semianalytic or computational. One can show by such semiquantitative analyses that two phenomena occur as the shock velocity increases. First, T_{ps} becomes approximately equal to the final downstream temperature T_{f}. Second, the precursor develops a diffusive structure, causing the second derivative of temperature with optical depth to change sign in the region near the density jump, becoming concave downward for strong-enough shocks. It has been asserted, with various degrees of definiteness in the aforementioned books and subsequent papers, that there is a "critical shock velocity" that divides regimes in which $T_{\mathrm{ps}} < T_{\mathrm{f}}$, and the precursor temperature T_{p} decays exponentially with optical depth, from those in which $T_{\mathrm{ps}} = T_{\mathrm{f}}$ and the precursor has a diffusive zone. One can approximately exclude the case $T_{\mathrm{ps}} > T_{\mathrm{f}}$ on thermodynamic grounds (as is discussed further below). More recently, Michaut *et al.* have evaluated the behavior of various atomic species under conditions relevant to OTR shocks, showing that in certain regimes they can produce comparatively large (> 10) increases in density [25].

Simulations of OTR shocks began in the 1960s with the well-known work of Heaslet and Baldwin [26]. Such shocks have been and will be a subject of simulation studies because their vast range of spatial scales represents a serious challenge for radiation hydrodynamic computational methods. Simulations of these shocks since the 1960s are rather sparse, [27]–[32] save for the work on line-transport-dominated shocks mentioned above. This no doubt reflects the computational challenges posed by the vast range of spatial scales present, the difficulty of observing astrophysical shocks that are not thin, and the paucity of experimental data for validation. Currently, the experiments previously mentioned are beginning to provide data, and the astrophysics community is actively developing advanced radiation-hydrodynamic codes, so we can expect to see much more work in this area in the near future.

However, because of their limited numerical accuracy, simulations are not always the best way to address conceptual issues in shock structure. For simple assumptions, semianalytic theory can provide exact solutions of the relevant equations and may prove able to conclusively demonstrate some causal connections within such systems. This has the additional benefit of providing, in some cases, exact solutions by which simulation methods and implementations can be verified. In this paper, we are concerned with the exploration of the properties and structure of OTR shocks based on exact fluid-dynamic equations and fundamental physical arguments. The result should prove useful for the evaluation of shock regimes in experiments and in astrophysics, for the design of experiments, and for identifying the conditions that may permit the most demanding comparison of experiment and simulation.

II. Theoretical Context

The radiative shocks of interest here occur in regimes where the matter can be described by fluid equations. For shocks embedded deep within optically thick media, one can begin by taking the point of view that the entire shock structure exists as an infinitesimal layer within the system, and that there is no need to distinguish among the various fluids (radiation, ion, electrons). The fluid equations for continuity, momentum, and energy, for planar shocks, by the standard calculation, [23], [33] then directly imply a set of Rankine–Hugoniot relations

$$\rho u = -\rho_{\mathrm{o}} u_{\mathrm{s}} \tag{1}$$

$$\begin{aligned} \rho u^2 + p &= -(\rho_{\mathrm{o}} u_{\mathrm{s}}) u + p \\ &= \rho_{\mathrm{o}} u_{\mathrm{s}}^2 + p_{\mathrm{o}} \end{aligned} \tag{2}$$

$$F_{\mathrm{R}} + \frac{\gamma}{\gamma-1} p u + \frac{\rho u^3}{2} = -\frac{\rho_{\mathrm{o}} u_{\mathrm{s}}^3}{2} - \frac{\gamma}{\gamma-1} p_{\mathrm{o}} u_{\mathrm{s}} + F_{\mathrm{Ro}}. \tag{3}$$

Here, ρ, u, p, and F_{R} designate the density, velocity, pressure, and radiation flux, respectively, with additional subscripts when needed as defined above. In the OTR shock, one has $F_{\mathrm{Ro}} = 0$ by the definition of the context. In addition, the material is assumed to be a polytropic gas with an internal energy density of $p/(\gamma - 1)$. The radiation flux is taken to be positive in the upstream direction, and the incoming flow is taken to have a negative velocity, with u_{s} being a positive number. Oblique shocks or shocks in curvilinear geometry introduce geometric complexity but no new conceptual elements. Because of this, we work herein with planar shocks whose shock surface is perpendicular to their velocity, taken to lie in the z-direction.

When we consider the transport of radiation, in later sections, we work within the context of the radiative transfer equation expressed as

$$\frac{1}{c}\frac{\partial I_{\mathrm{R}}}{\partial t} + \frac{\partial I_{\mathrm{R}}}{\partial s} = \int \kappa_\nu (B_\nu - I_\nu) d\nu + \int \sigma_\nu (J_\nu - I_\nu) d\nu \tag{4}$$

in which the radiation intensity (energy flux per steradian) is I_{R}, the path of the radiation is described by s, c is the speed of light, and the integrals are over all frequencies ν. The integral of I_ν over all frequencies is I_{R}. Within the integrals, the subscript ν indicates spectral dependence with units as appropriate. The functions involved are the absorption opacity κ_ν, the scattering opacity σ_ν, the spectral thermal intensity (the Planck function) B_ν, the spectral radiation intensity I_ν, and the mean of the spectral intensity over all solid angle J_ν. This equation is written in the geometric-optics limit, which is relevant to radiative shocks, and under the assumption that the scattering is elastic and isotropic. It can be viewed fundamentally as a kinetic equation for the photons. Because the radiation within any distribution of matter reaches steady state instantaneously on the timescales of material motion, we will work with the time-independent version of this equation. The integral of (4) over all solid angle then gives

$$\partial F_{\mathrm{R}}/\partial z = 4\pi\kappa_{\mathrm{p}}(B - J_{\mathrm{R}}) \tag{5}$$

in 1-D, in which $J_{\mathrm{R}} = \int_{4\pi} I_{\mathrm{R}} d\Omega/(4\pi)$, $\mathbf{F}_{\mathrm{R}} = \int_{4\pi} I_{\mathrm{R}}\mathbf{n} d\Omega/(4\pi)$, and $B = \sigma T^4/\pi$, where $\mathbf{n}$ is the unit direction vector, a Stefan-Boltzmann constant σ, and a Planck mean opacity κ_{p}, assumed as usual to be accurate for J_{R} in addition to B.

From the theoretician's point of view that the entire shock is an infinitesimal layer, one would be interested primarily in evaluating the relation between initial and final states under various assumptions. However, reality often intrudes on this point of view by breaking its assumptions. We will see that the radiative component of the shock structure can easily be hundreds of radiation mean-free paths or more in extent. More generally, if one takes the point of view that the precursor is a Marshak-like wave driven by the shock-heated material, one can show [33] that the length of the precursor scales as u_{s} to a large power. In real systems such as stellar atmospheres, [12] a modest variation in shock velocity can cause the shock transition to expand to a scale larger than that of the system of interest, so that the shock enters a different regime. One such regime, relevant also to some current experiments, [8] is that in which the shocked matter remains optically thick while the upstream region is optically thin. This motivates an examination of the actual structure of OTR shocks, which among other consequences, will allow one to see when they do transition to some other regime.

The decision to examine the shock structure alters the context underlying (1)–(3) above. These equations describe the conservation of mass, momentum, and energy between any two points in an extended system only if it is in steady state. To obtain a specific tractable problem, we are thus forced to consider systems that are in steady state at least when measured by the time it takes the matter in the system to flow through the entire shock structure. Other simple problems, beyond our scope here but potentially of interest, would include the behavior in systems with known time dependence such as shocks accelerating down stellar density gradients or blast waves moving through a constant-density medium.

The decision to examine the shock structure must also prompt a re-examination of the point of view that the system may be treated as a single fluid. This examination has been carried out in books [14], [23], [33] and in the literature that preceded them. Here, we summarize the results. The ions are heated by viscosity on the smallest scale, over which any abrupt increase in density occurs. The direct electron heating on this scale is small. The next larger scale is the scale of ion-electron energy exchange, which heats the electrons and further ionizes the ions until the ion and electron temperature become equal. The radiative-cooling scale, in the shocked heated matter, is typically larger than this. Under common conditions, the rate of electron cooling by radiation is smaller than the rate of electron heating by collisions with ions. This is expected as, for any frequency, the radiative cooling rate by bremsstrahlung is smaller than the electron-ion collision rate by the square of the ratio of the electron plasma frequency to the radiation frequency, which is a small number for all frequencies of interest. When line emission is important, this can impact the detailed structure of the electron-heating region [34]. Despite being much larger than the electron-heating scale, the size of the cooling layer remains small in units of the radiation optical depth for reasons discussed below. The largest scale is that of the radiative precursor, which is a minimum of one radiation optical depth in extent and is often much larger than this. In the following discussion, we will assume that the density jump and electron-ion equilibration occur on an infinitesimal scale, and concern ourselves only with the structure introduced by the emission and absorption of radiation.

The fluid dynamics of an OTR shock determines much regarding its structure, independent of any and all details of the radiation transport. Although some books and even some recent papers treat the fluid dynamics approximately, it is in actuality not difficult to treat it exactly. Naturally, simulations should be compared to the exact solutions. Under our assumptions here, (1)–(3) express the fluid-dynamic constraints imposed by the conservation of mass, momentum, and energy. From these equations, one can derive the following simple normalized expressions showing the relative variation of the fluid-dynamic quantities. The effective independent variable is the inverse compression $\eta = \rho_{\mathrm{o}}/\rho$, which in all cases has a value between 0 and 1. We use the subscript n for normalized quantities. The natural normalization of the pressure is the ram pressure $\rho_{\mathrm{o}} u_{\mathrm{s}}^2$, so $p_{\mathrm{n}} = p/\rho_{\mathrm{o}} u_{\mathrm{s}}^2$. One can show

$$p_{\mathrm{n}} = (1 - \eta) + p_{\mathrm{on}}. \tag{6}$$

The temperature in isolation is rather cumbersome to work with, while in contrast, the specific pressure $p/\rho = RT$, in which R is the usual gas "constant," proves convenient. Note that R certainly may not be constant in systems of interest. The natural normalization of RT is $RT_{\mathrm{n}} = RT/u_{\mathrm{s}}^2$, and one has

$$RT_{\mathrm{n}} = \eta(1 - \eta) + p_{\mathrm{on}}\eta. \tag{7}$$

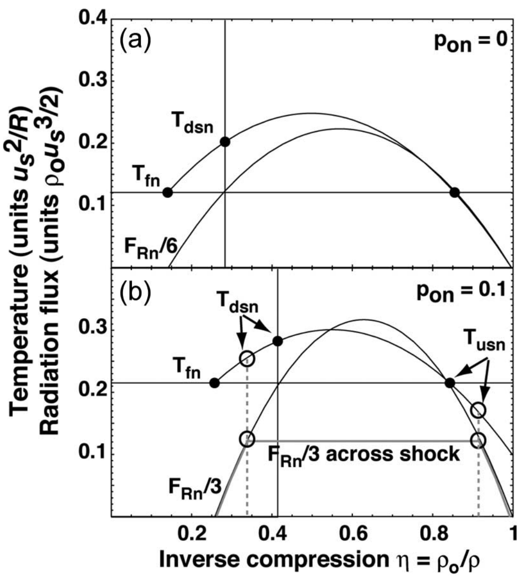

Fig. 2. Profiles of normalized temperature and radiation flux, scaled to cross at the maximum upstream precursor temperature, for $\gamma = 4/3$ and constant R. The leftmost solid dots show the normalized final temperature (which does not vary with shock strength). The center solid dots shows the maximum postshock temperature, which is $(3-\gamma)T_{\mathrm{fn}}$. The rightmost solid dots show the maximum preshock temperature in the precursor. (a) For $p_{\mathrm{on}} = 0$. (b) For $p_{\mathrm{on}} = 0.1$. Here, the open circles show one possible shock, in which the precursor compresses and heats up to some temperature T_{usn}. The density jump is determined by the requirement of constant radiation flux, and the immediate postshock temperature is between T_{dsn} and T_{fn}.

The natural normalization of the radiation flux is simply shown to be $F_{\mathrm{Rn}} = 2F_{\mathrm{R}}/(\rho_{\mathrm{o}} u_{\mathrm{s}}^3)$. Thus, the normalized radiation flux is the ratio of the physical radiation flux to the incoming kinetic energy flux from upstream. Equation (3) together with (6) and (7) then implies

$$F_{\mathrm{Rn}} - F_{\mathrm{Ron}} = -1 - \frac{\gamma+1}{\gamma-1}\eta^2 + \frac{2\gamma}{\gamma-1}\left[\eta - p_{\mathrm{on}}(1-\eta)\right] \tag{8}$$

where in the OTR shock, one has $F_{\mathrm{Ron}} = 0$. The author suggests that the formulation above, in which the initial upstream pressure becomes a parameter that might be zero, is frequently more useful that a formulation in terms of an upstream Mach number (or some sort of "Boltzmann number" relating a thermal radiation flux to an upstream or downstream temperature). One reason is that it is the upstream kinetic energy that drives the radiative dynamics. Another reason is that the upstream pressure becomes negligibly important for strong-enough shocks, and radiative shocks are most often quite strong. A third reason is that the relevant simple limit of zero upstream pressure follows naturally.

Fig. 2 shows the implications of (7) and (8) for the shock structure. These equations are evaluated for $\gamma = 4/3$ in this figure, which is a reasonable estimate [33] for ionizing media. As matter enters the precursor from the right, radiation absorption decreases the radiation flux and increases the pressure, which in turn slows the flow and drives the density up (and thus η down). At some inverse compression, the density jumps. The specific density where the jump occurs is determined by the requirement that the detailed shock structure must ultimately be consistent with the global conservation of momentum and energy, as is discussed below. The density jump is subject to the physical requirement that the radiation flux cannot change across it. The immediate postshock temperature T_{ds} is necessarily higher than the immediate preshock temperature T_{us}. Downstream of the density jump, the plasma cools and the net radiation flux decreases until the radiation flux reaches zero at the final temperature T_{f}. The final values of η_{f} and RT_{fn} are implied by the requirement that F_{R} be zero there, and are

$$\eta_{\mathrm{f}} = \frac{\gamma-1}{\gamma+1} + \frac{2\gamma}{\gamma+1}p_{\mathrm{on}} \tag{9}$$

and

$$RT_{\mathrm{fn}} = \frac{2(\gamma-1)}{(\gamma+1)^2}\left[1 + \frac{\gamma p_{\mathrm{on}}}{2} + \gamma p_{\mathrm{on}}^2\right] + \frac{5\gamma-1}{(\gamma+1)^2}p_{\mathrm{on}} \tag{10}$$

respectively.

The detailed behavior at an actual density jump is of course more complicated than it would be for an infinitesimal jump. In real systems, there may be some electron heating, some ionization, and some radiation during the actual transition [34] and also further ionization and some radiation while the electron and ion temperatures equilibrate.

Fig. 2 also shows the relation of the parameters for the case that $T_{\mathrm{us}} = T_{\mathrm{f}}$. Landau and Lifshitz argue that the case $T_{\mathrm{us}} > T_{\mathrm{f}}$ is thermodynamically prohibited. Their view is that radiation from the shocked matter carries energy upstream at temperature T_{f} while the heated plasma and radiation from the (optically very thick) precursor carry this same energy back across the density jump at temperature T_{us}. The value of this "recycled" energy flux at any location is the negative of the net local upstream radiation flux F_{R}–F_{Ro}. If T_{us} were greater than T_{f}, then this transport of heat would create a decrease in entropy, which is disallowed by the second law of thermodynamics. This argument is not quite correct as it ignores the flow of energy and entropy from the cooling layer, which is at higher temperature. The thermodynamic limit is actually

$$\frac{1}{T(\tau=0)} \geq \frac{1}{[F_{\mathrm{R}}(\tau=0) - F_{\mathrm{Ro}}]}\int_0^\infty \frac{1}{T(\tau)}\left(\frac{\partial F_{\mathrm{R}}(\tau)}{\partial \tau}\right)e^{-\tau}d\tau \tag{11}$$

where F_{R} is the local value of the radiation flux and τ is the optical depth measured downstream relative to any point of interest. Note that if T were constant and equal to T_{f} then this equation would imply $T_{\mathrm{us}} \leq T_{\mathrm{f}}$. In reality, $T > T_{\mathrm{f}}$ throughout the cooling layer, and so thermodynamically T_{us} can be greater than T_{f} by some small amount. The amount turns out to become comparatively negligible in the limit of very strong shocks. Because the system exists near the limiting state where $T_{\mathrm{us}} = T_{\mathrm{f}}$ over a wide range of parameters, the properties of this state are worth knowing. The limiting upstream and downstream values of η across the density jump are

$$\eta_{\text{us}}\big|_{T_{\text{us}}=T_{\text{f}}} = \frac{2}{\gamma+1} - p_{\text{on}}\frac{\gamma-1}{\gamma+1} \tag{12}$$

and

$$\eta_{\text{ds}}\big|_{T_{\text{us}}=T_{\text{f}}} = 2\frac{\gamma-1}{\gamma+1} + p_{\text{on}}\frac{3\gamma-1}{\gamma+1} \tag{13}$$

respectively, while the limiting value of the immediate postjump temperature is

$$RT_{\text{dsn}}\big|_{T_{\text{us}}=T_{\text{f}}} = \frac{2(\gamma-1)}{(\gamma+1)^2}\left[(3-\gamma) - p_{\text{on}}^2(3\gamma-1) - p_{\text{on}}\frac{18\gamma-7(\gamma^2+1)}{2(\gamma-1)}\right]. \tag{14}$$

One can see that for $p_{\text{on}} = 0$, the limiting ratio of RT_{dsn} to RT_{fn} is $(3-\gamma)$.

This limiting case is not accessible if η_{us} from (2) is less than the maximum of the radiation flux curve, which is at

$$\eta_{\text{max}} = \frac{\gamma}{\gamma+1}(1+p_{\text{on}}). \tag{15}$$

Thus, the limiting case is not accessible for $p_{\text{on}} > (2-\gamma)/(2\gamma-1)$. Since $p_{\text{on}} = 1/(\gamma M^2)$, where M is the traditional upstream Mach number, this corresponds to

$$M < \sqrt{\frac{2\gamma-1}{\gamma(2-\gamma)}} \tag{16}$$

which is 1.4 for $\gamma = 4/3$ and 2 for $\gamma = 5/3$.

III. Energy Balance in a Three-Layer Model

In this section, we investigate the implications of energy balance for the shock structure. We use a three-layer approximation to the structure near the density jump and thus ignore the adaptation zones. We will describe this as a three-layer model. No analytic or semianalytic work has yet attempted a five-layer model, as would be needed to account for the adaptation zones. As discussed above, three-layer models cannot account for the (small) effects of radiation transport over the first few optical depths near the cooling layer. The specific implication is that the upstream temperature in such a model refers to the temperature in the precursor beyond the adaptation zone. We will designate this temperature T_{ps}. Within this context, one can usefully specify the balance of energy fluxes at the two locations illustrated in Fig. 3. Designating the radiative flux from the cooling layer (equal in both directions because the cooling layer turns out to be optically very thin) as the positive number F_{cl} and that from the precursor region as F_{Rp} (which is negative), we can note that the net radiation flux must be zero at the boundary where the system reaches its final downstream state. This gives

$$\sigma T_{\text{f}}^4 - F_{\text{cl}} + F_{\text{Rp}}(1-\tau_{\text{cl}}) = 0 \tag{17}$$

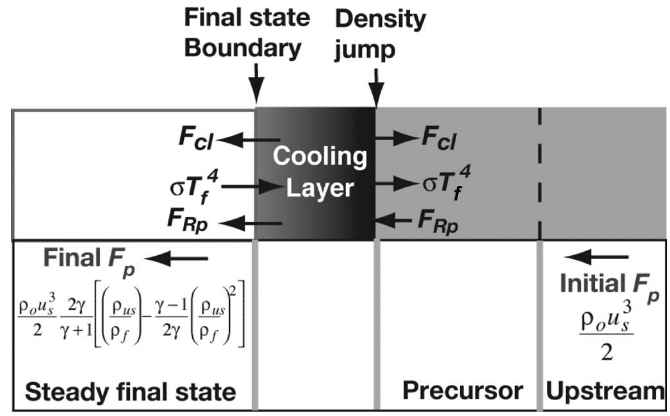

Fig. 3. Schematic of energy balance in OTR shocks, showing the density jump and the final state boundaries where (17) and (18) apply.

in which the optical depth of the cooling layer, assumed small as confirmed below, is τ_{cl}, and so the transmission through the cooling layer can be written as $(1-\tau_{\text{cl}})$. There is a net energy flux through the density jump that equals the initial value entering from upstream. All the other energy fluxes through this point must balance to zero. This gives

$$\sigma T_{\text{f}}^4(1-\tau_{\text{cl}}) + F_{\text{cl}} + F_{\text{Rp}} + F_{\text{p}} = 0 \tag{18}$$

in which

$$F_{\text{p}} = \frac{\gamma}{\gamma-1}pu + \frac{\rho u^3}{2} + \frac{\rho_{\text{o}} u_{\text{s}}^3}{2} + \frac{\gamma}{\gamma-1}p_{\text{o}} u_{\text{s}} \tag{19}$$

is the (negative) flux of plasma energy due to the heating in the precursor. That is, F_{p} is the total plasma energy flux less the initial value, which, for $p_{\text{o}} = 0$, is $-\rho_{\text{o}} u_{\text{s}}^3/2$. Taken together, these relations imply that

$$F_{\text{cl}} = -F_{\text{p}}\frac{(1-\tau_{\text{cl}})}{(2-\tau_{\text{cl}})} + \tau_{\text{cl}}\sigma T_{\text{f}}^4. \tag{20}$$

The implication of (18) and (20) is that $-F_{\text{Rp}} < \sigma T_{\text{f}}^4$ always, because F_{p} is always finite. Specifically, by substituting for the pressure in (19), one can show that

$$F_{\text{p}}\big|_{M\to\infty} = -\frac{\rho_{\text{o}} u_{\text{s}}^3}{2}\frac{(5+\gamma)}{(\gamma+1)} \tag{21}$$

which one finds to be the same on either side of the density jump as it should be.

It is helpful to define a shock strength parameter Q as

$$Q = 2\sigma u_{\text{s}}^5/(R^4\rho_{\text{o}}). \tag{22}$$

This implies that the normalized radiation flux flowing upstream from the final state is

$$\sigma T_{\text{f}}^4/(\rho_{\text{o}} u_{\text{s}}^3/2) = 16Q(\gamma-1)^4/(\gamma+1)^8. \tag{23}$$

The choice of a shock strength parameter has the advantage that it excludes powers of γ that might be replaced by quantities involving some other approach to the equation of state, but the disadvantage that Q must be large to enter the radiative regime.

Specifically, to make the normalized radiation flux equal to 1 requires $Q = 5000$ for $\gamma = 4/3$ and $Q = 800$ for $\gamma = 5/3$.

One can now estimate the optical depth of the cooling layer for large Mach number by approximating $F_{\rm cl}$ as $\tau_{\rm cl}\sigma T_{\rm ds}^4$, which becomes $\tau_{\rm cl}(3-\gamma)^4\sigma T_{\rm f}^4$. Using (20)–(22), one finds for large Q that

$$\tau_{\rm cl}|_{M\to\infty} = \frac{(\gamma+1)^7(5+\gamma)}{32Q(3-\gamma)^4(\gamma-1)^4} \tag{24}$$

which is $\sim 780/Q$ for $\gamma = 4/3$ and $\sim 320/Q$ for $\gamma = 5/3$. The implication is that the plasma flux $F_{\rm p}$ and the cooling layer flux $F_{\rm cl}$ both tend toward constant values as the shock becomes very strong, while the radiation fluxes from the downstream and upstream heated matter increase in proportion to Q.

The energy balance can further be used to develop a first relation between $T_{\rm ps}$ and $T_{\rm f}$. One can write $T_{\rm ps} = f_{\rm s}T_{\rm f}$ and $F_{\rm Rp} = -\varepsilon_{\rm p} f_{\rm s}^4\sigma T_{\rm f}^4$, where $\varepsilon_{\rm p}$ is the effective emissivity of the precursor, assumed to be 1 in the traditional treatments on the assumption that the precursor is optically very thick. Then, the limiting value of $(1-\varepsilon_{\rm p}f_{\rm s}^4)$, for large enough Q that $\tau_{\rm cl}$ can be neglected in (18) and (20), is $(3-\gamma)(\gamma+1)^7/(32Q(\gamma-1)^4)$, so $f_{\rm s}$ and $\varepsilon_{\rm p}$ cannot both be 1.

Having set $T_{\rm ps} = f_{\rm s}T_{\rm f}$, one can find the value of η corresponding to this temperature in the precursor, and one can evaluate $F_{\rm p}$ (and hence $F_{\rm cl}$) for this η. One can then use (1)–(8) to find $\eta_{\rm ds}$ and $\eta_{\rm us}$ (and thus $\rho_{\rm ds}$, $\rho_{\rm us}$, $T_{\rm ds}$, $T_{\rm ps}$, and $F_{\rm R}$) and can use the energy balance to obtain the relation between $f_{\rm s}$ and Q, given by

$$Q = \frac{(\gamma+1)^7}{64\,(1-\varepsilon_{\rm p}f_{\rm s}^4)\,(\gamma-1)^4} \times \left[4f_{\rm s} + (\gamma+1)\left(-1+\sqrt{1-8f_{\rm s}\frac{(\gamma-1)}{(\gamma+1)^2}}\right)\right]. \tag{25}$$

In fact, within this three-layer-model context, neither $f_{\rm s}$ nor $\varepsilon_{\rm p}$ can be 1 although both asymptotically approach it. The divergence of the radiation flux ($\partial F_{\rm R}/\partial z$ here) must be nonzero immediately upstream of the adaptation zone, otherwise the precursor would not evolve as one moves further upstream. This has the implication through (7) and (8) that there must be a gradient in temperature and thus that $\varepsilon_{\rm p} < 1$. The approach to 1 of $\varepsilon_{\rm p}$ (from below) is controlled by the decrease of the temperature gradient in the precursor, which behaves like a Marshak radiation wave from a moving source [33]. The dependence of $\varepsilon_{\rm p}$ on $u_{\rm s}$ is determined by this behavior and thus not as would be demanded by (25) if $f_{\rm s}$ were 1. The implication is that $f_{\rm s}$ as defined here in the region beyond the upstream adaptation zone must approach 1 from below as Q increases. In contrast, ongoing numerical work by John Castor suggests that the temperature inside the adaptation zone, at the actual density jump, may be pulled up above $T_{\rm f}$.

IV. Cooling Layer Structure

The structure of the cooling layer can be determined using (5) and the derivative of (8), if one can find a way to solve for $J_{\rm R}$. A diffusion model cannot accurately capture the structure of $J_{\rm R}$ in and near the cooling layer, because substantial changes in thermal intensity occur on a distance small compared to an optical depth. The author has argued elsewhere [35] that $J_{\rm R}$ can be approximated to good accuracy as constant through the cooling layer, and that this approximation becomes more accurate as the shock strength increases. This is a consequence of the small optical depth of and limited temperature increase in the cooling layer. Within this approximation, and in the context of a three-layer model, matching the cooling layer to the final state requires $J_{\rm R} = B_{\rm f} = \sigma T_{\rm f}^4/\pi$.

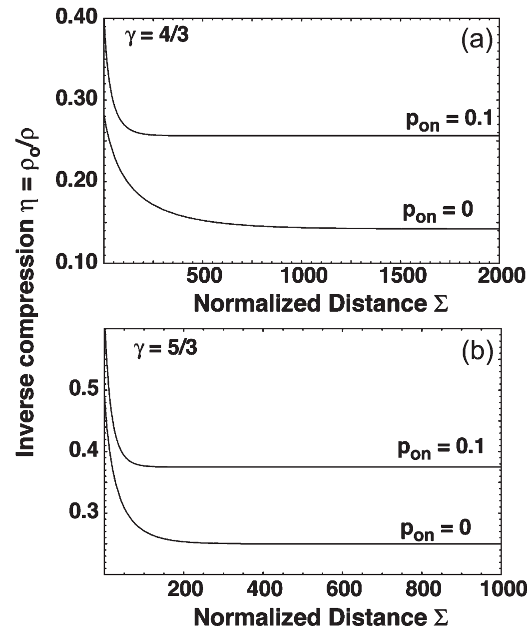

Fig. 4. Universal profiles of the inverse compression in the cooling layer versus the normalized distance $\Sigma_{\rm ds}$ with $d\Sigma_{\rm ds} = -\kappa_{\rm p}Q dz$. The shock is on the left. Note that since $Q \gg 1000$ for strongly radiative shocks, the cooling layer is much less than one optical depth in extent.

The calculation of the cooling layer profile within such a model is straightforward. The derivative of (8) gives

$$\frac{\partial F_{\rm Rn}}{\partial z} = \left(-2\frac{\gamma+1}{\gamma-1}\eta + \frac{2\gamma}{\gamma-1}[1+p_{\rm on}]\right)\frac{\partial \eta}{\partial z} \tag{26}$$

which one can set equal to (5). In addition, one knows $RT_{\rm fn}$ through (10) therefore one knows $B_{\rm f} = J_{\rm R}$, and one knows $RT_{\rm n}$ through (7), so one knows B as a function of η. One specifically obtains

$$\frac{\partial F_{\rm Rn}}{\partial z} = 4Q\kappa_{\rm p}\left[(1+p_{\rm on}-\eta)^4\eta^4 - \frac{\left(2p_{\rm on}^2\gamma(\gamma-1)+p_{\rm on}(\gamma^2-6\gamma-1)-2(\gamma-1)\right)^4}{(\gamma+1)^8}\right]. \tag{27}$$

One can combine (26) and (27) and integrate to obtain $\eta(z)$. This traditionally is done in terms of optical depth $\tau_{\rm ds}$ defined by $d\tau_{\rm ds} = \pm\kappa_{\rm p} dz$. The $\pm$ here refers to the fact that the integral can proceed either from the shock or from an infinitesimal perturbation from the final state, with equal results. Note, however, that in reality, the quantity $(Q\kappa_{\rm p})$ sets the distance scale. For any given value of γ and of $p_{\rm on}$, there is a universal

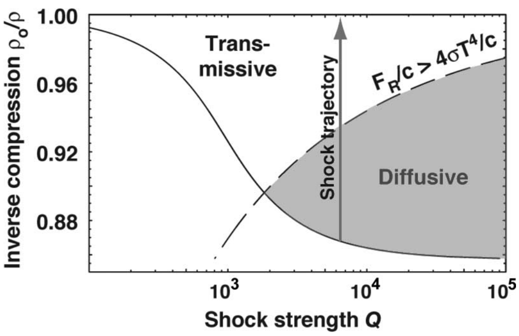

Fig. 5. Value of the precursor inverse compression η_{us} at the shock (solid) and the boundary (dashed) above which the local emission contributes negligibly to radiation flux. The arrow shows the upstream trajectory of the system for one value of Q. These specific curves are for $\gamma = 4/3$ and $p_{\mathrm{o}} = 0$. The solid curve also assumes $\varepsilon_{\mathrm{p}} = 1$.

shape to this curve as a function of a variable Σ_{ds} defined by $d\Sigma_{\mathrm{ds}} = \pm\kappa_{\mathrm{p}} Q dz$. Fig. 4 shows some examples, with $\Sigma_{\mathrm{ds}} = 0$ defined as the value of η where $T_{\mathrm{ps}} = T_{\mathrm{f}}$ (i.e., $f_{\mathrm{s}} = 1$). In any actual shock, with some value of $f_{\mathrm{s}} < 1$, the portion of the curve to the right of the point where $\eta = \eta_{\mathrm{ds}}$ will apply. The calculation just described determines the profile of the cooling layer but does not determine the values of the parameters at the density jump (i.e., it does not determine f_{s}). We discuss below how to match the solution for the cooling layer with one for the precursor. In actual shocks, the deviation of J_{R} from constant will cause the cooling layer profiles to vary with Q. In addition, any spatial variation of Q and κ_{p} as density and temperature vary will cause the shape of the cooling layer in space to appear different from these curves.

V. Precursor Regimes and Structure

The precursor region has regimes that are once again readily identified from the fluid dynamics of the system. Beyond some distance from the shock, one enters the transmissive region in which $F_{\mathrm{R}}/c > 4\sigma T^4/c$, so the energy density associated with the radiation flux is large compared to that associated with local thermal emission. This is implied by the fluid dynamics and thus is unavoidable. One can, for example, determine from (7) and (8) the value of Q for which the system will be in the transmissive region for $1 \geq \eta > \eta_t$, finding

$$Q = \frac{(\eta_t - 1)\left[(\gamma+1)\eta_t - (\gamma-1) - 2\gamma p_{\mathrm{on}}\right]}{4(\gamma-1)\eta_t^4(1-\eta_t+p_{\mathrm{on}})^4}. \tag{28}$$

In this region, the emission from the precursor becomes negligible, and the radiation becomes beamlike within very few absorption lengths because increasingly oblique rays are increasingly absorbed. Then, $F_{\mathrm{R}} = cE_{\mathrm{R}}$ and so attenuates exponentially with optical depth. Fig. 5 shows schematically how η_{us} and the boundary of this region depend on Q, using (25) in the approximation that the precursor emissivity $\varepsilon_{\mathrm{p}} = 1$. For any Q, η in the precursor moves from the solid curve at the density jump upward to 1 at the upstream limit of the precursor. Whatever portion of the precursor is above the dashed line is in the transmissive region.

The region below the dashed line in Fig. 5 can be described as the diffusive region. It is evident from Fig. 5 that this region is at first quite narrow, becoming wider as Q increases. Beyond the adaptation zone, one can obtain a solution for the precursor profile using a nonequilibrium-diffusion model with

$$F_{\mathrm{R}} = -(f_{\mathrm{E}}4\pi/\overline{\chi})\partial J_{\mathrm{R}}/\partial z \tag{29}$$

in which $\overline{\chi}$ is an opacity approximately equal to the Rosseland mean opacity, and f_{E} is an Eddington factor. Note that the radiation energy density E_{R} is $4\pi J_{\mathrm{R}}/c$. The Eddington factor is the ratio of radiation pressure to the radiation energy density. It is 1/3 for isotropic radiation, 1 for beaming radiation, and $< 1/3$ for radiation having a "pancaked" angular distribution. In the transmissive region, $F_{\mathrm{R}} = 4\pi J_{\mathrm{R}}$, in which case (29) gives the exponential decrease of the mean intensity with distance in this region. Equation (29) also makes possible a calculation of the precursor structure as follows. Using this radiation flux in (8) and the transport model in (26), one obtains coupled differential equations for J_{R} and η. We normalize J_{R} as we did F_{R} to the incoming kinetic energy, so $J_{\mathrm{Rn}} = J_{\mathrm{R}}/(\rho_{\mathrm{o}} u_{\mathrm{s}}^3/2)$

$$1 - \frac{2\gamma}{\gamma-1}\left(\eta - p_{\mathrm{on}}(1-\eta)\right) + \frac{\gamma+1}{\gamma-1}\eta^2 - f_{\mathrm{E}}\frac{4\pi}{\overline{\chi}}\frac{\partial J_{\mathrm{Rn}}}{\partial z} = 0 \tag{30}$$

and

$$2\kappa_{\mathrm{p}}\left[\pi J_{\mathrm{Rn}} - Q(\eta-1)^4\eta^4\right] = \left[\frac{\eta(\gamma+1) - \gamma(1+p_{\mathrm{on}})}{\gamma-1}\right]\frac{\partial\eta}{\partial z}. \tag{31}$$

The implications of these equations merit some discussion. Note that f_{E} and $\overline{\chi}$ appear only in their ratio. This might lead one to hope to find a universal shape for the precursor, but the term in (31) involving κ_{p} prevents this. If one multiplies (31) by $f_{\mathrm{E}}/\overline{\chi}$ and defines an effective optical depth variable $\tau_{\mathrm{eff}} = -\overline{\chi}z/f_{\mathrm{E}}$, with the sign corresponding to integration toward the density jump, then one obtains (32) and (33) containing the parameters p_{on}, Q, and $\kappa_{\mathrm{p}} f_{\mathrm{E}}/\overline{\chi}$. One might hope to parameterize $\kappa_{\mathrm{p}} f_{\mathrm{E}}/\overline{\chi}$ as a function of η (and hence the other material properties). However, the Eddington factor f_{E} cannot be parameterized in this way. Here, one faces the limits of a semianalytic description at this level of approximation. We will model the diffusive region by taking $f_{\mathrm{E}} = 1/3$. This is accurate throughout the portion of the precursor that is in the diffusive region. The increase of f_{E} in the transmissive region will increase the length of this portion of the precursor relative to the result we will obtain. In addition, the treatment of the upstream adaptation zone will be inexact in this as in other respects, as $f_{\mathrm{E}} < 1/3$ there.

The resulting equations are

$$1 - \frac{2\gamma}{\gamma-1}\left(\eta - p_{\mathrm{on}}(1-\eta)\right) + \frac{\gamma+1}{\gamma-1}\eta^2 + 4\pi\frac{\partial J_{\mathrm{Rn}}}{\partial\tau_{\mathrm{eff}}} = 0 \tag{32}$$

and

$$2\frac{\kappa_{\mathrm{p}} f_{\mathrm{E}}}{\overline{\chi}}\left[\pi J_{\mathrm{Rn}} - Q(\eta-1)^4\eta^4\right] + \left[\frac{\eta(\gamma+1) - \gamma(1+p_{\mathrm{on}})}{\gamma-1}\right]\frac{\partial\eta}{\partial\tau_{\mathrm{eff}}} = 0. \tag{33}$$

The behavior of these equations becomes more clear if one restates them in terms of $\varepsilon = 1 - \eta$, which is always small and approaches zero at the upstream edge of the precursor. This gives for $p_{\text{on}} = 0$

$$\frac{\varepsilon}{\gamma - 1}\left(\varepsilon(\gamma + 1) - 2\right) + 4\pi\frac{\partial J_{\text{Rn}}}{\partial \tau_{\text{eff}}} = 0 \tag{34}$$

and

$$2\frac{\kappa_{\text{P}} f_{\text{E}}}{\overline{\chi}}\left[\pi J_{\text{Rn}} - Q(1-\varepsilon)^4\varepsilon^4\right] - \left[\frac{1-\varepsilon(\gamma+1)}{\gamma-1}\right]\frac{\partial \varepsilon}{\partial \tau_{\text{eff}}} = 0 \tag{35}$$

while the relation between J_{Rn} and ε in the transmissive region where the radiation flux is beamlike is

$$J_{\text{Rn}} = \frac{\varepsilon\left(2 - \varepsilon(\gamma + 1)\right)}{4\pi(\gamma - 1)}. \tag{36}$$

Some aspects of these equations deserve comment. First, near the upstream edge of the precursor, ε increases exponentially as does J_{Rn}. Second, the first term in square brackets on the left-hand side of (35) must always be positive (for positive J_{R}). Near the upstream end of the precursor, it is evident that J_{Rn} dominates this term. It would decrease to zero only if local thermodynamic equilibrium were reached identically, which never can happen within a radiative shock that must carry a finite net radiation flux. Yet, the larger Q becomes, the sooner the precursor reaches the diffusive region as ε increases and the smaller the left term in (33) becomes. This has the implication that the precursor becomes longer.

A third aspect of these equations is that the transition from the transmissive to the diffusive region is controlled by the additional parameter $\kappa_{\text{P}} f_{\text{E}}/\overline{\chi}$. As this parameter decreases, the increase in ε occurs more slowly. This both delays the onset of the diffusive region and slows the increase in J_{R}. Fig. 6 illustrates this by showing the behavior of ε and J_{Rn} implied by (34) and (35). Here, the display is arbitrarily terminated at the limits of the graphs. In the actual shock, the length of the precursor is established by the matching requirements discussed in the next section. The curves in Fig. 6(a) showing ε are concave upward in the transmissive region and transition to concave downward in the diffusive region. In the limit of very large $\kappa_{\text{P}} f_{\text{E}}/\overline{\chi}$, although this is not likely physically, the precursor would quickly enter the diffusive region and reach a minimum length for any specific Q.

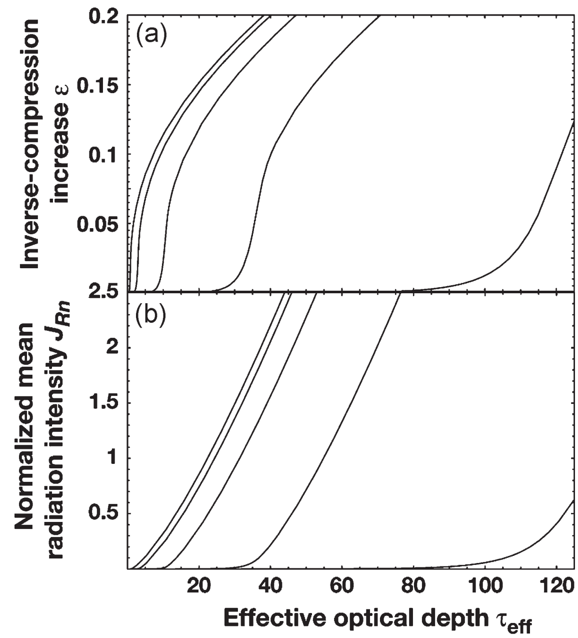

Fig. 6. Structure of precursor as $\kappa_{\text{P}} f_{\text{E}}/\overline{\chi}$ varies, for $Q = 10\,000$, $\gamma = 4/3$, and $p_{\text{on}} = 0$. (a) Inverse-compression increase, $\varepsilon = 1 - \eta$, is plotted against τ_{eff}, for $\kappa_{\text{P}} f_{\text{E}}/\overline{\chi} = 0.1, 1, 10, 100,$ and 1000. Larger $\kappa_{\text{P}} f_{\text{E}}/\overline{\chi}$ is to the left. (b) Normalized mean radiation intensity J_{Rn} is plotted against τ_{eff}, for $\kappa_{\text{P}} f_{\text{E}}/\overline{\chi} = 0.1, 1, 10, 100,$ and 1000. Larger $\kappa P f E/\overline{\chi}$ is to the left.

VI. Structure Calculations in the Three-Layer Model

One can complete a self-consistent calculation of the structure in the three-layer model as is described here and has been discussed more thoroughly elsewhere [35]. On the one hand, the approach described here is new and should be more accurate in the cooling layer than a calculation using nonequilibrium diffusion. On the other hand, the present calculation remains approximate, as the next section considers. The method of calculating the entire structure is as follows. It is sufficient to calculate the profile of the inverse compression for the reasons discussed in Section III. One begins by calculating the downstream profile as described in Section IV, from the limit corresponding to $T_{\text{ps}} = T_{\text{f}}$ to the final downstream state, whose properties depend only on Q and γ. This calculation does not determine the value of f_{s} or equivalently the actual value η_{ds} of the inverse compression at the downstream side of the density jump, which is smaller than the limiting value. It does determine the structure of the cooling layer, whose shape from η_{f} to any given $\eta < \eta_{\text{ds}}$ does not depend on η_{ds}. Thus, at this point, one knows the structure of the cooling layer but one does not know where the cooling layer ends.

One can find the end of the cooling layer and the parameters at the density jump by enforcing the continuity of J_{R} at the density jump. Throughout the cooling layer, $J_{\text{R}} = B_{\text{f}}$ from the assumption of constant J_{R} discussed in Section IV. At the density jump, J_{R} includes a contribution from the final state, from the cooling layer, and from the precursor. One can evaluate the downstream contribution J_{d} as

$$J_{\text{d}} = \frac{B_{\text{f}}}{2} + \frac{1}{2}\int_0^\infty \left(B(\tau) - B_{\text{f}}\right)\Gamma(0,\tau)d\tau \tag{37}$$

in which τ is the optical depth, increasing from the density jump toward the final state. The corresponding value of the contribution to J_{R} from the precursor is $J_u = B_{\text{f}} - J_{\text{d}}$. By evaluating J_{d} as η_{ds} varies, one thus obtains one evaluation of $J_u(f_{\text{s}})$ (any given value of η_{ds} corresponds to a given value of the temperature ratio $f_{\text{s}} = T_{\text{ps}}/T_{\text{f}}$).

Turning to the precursor structure, for any assumed value of f_{s}, and with values of Q, γ, p_{on}, and $\kappa_{\text{P}} f_{\text{E}}/\overline{\chi}$, one can use (32) and (33) [or (34) and (35)] to calculate the structure of the precursor from its upstream end to the density jump. One can repeat this calculation to determine $J_{\text{R}}(f_{\text{s}})$, the upstream

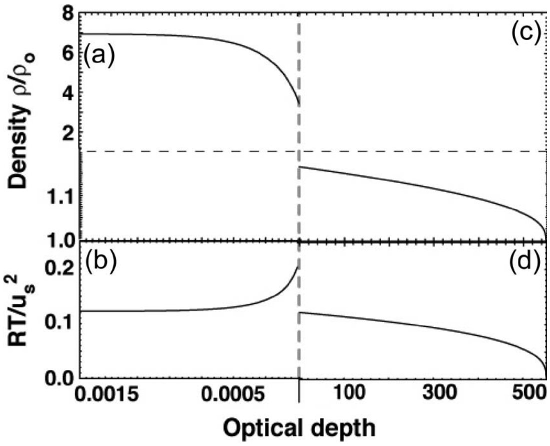

Fig. 7. Structure of an OTR shock for $Q = 10^6$, $\kappa_\mathrm{p} f_\mathrm{E}/\overline{\chi} = 1/3$, and $\gamma = 4/3$. The density jump occurs at the vertical dashed line, where the optical depth scales change. The optical depth scale of the (a) cooling-layer density and (b) temperature increases to the left from the density jump, while that of the (c) precursor density and (d) temperature increases to the right. The density scale changes at the horizontal dashed line.

portion of which must be equal to J_u. Here, we evaluate the upstream portion of J_R in the precursor as $J_\mathrm{R}/2$, assuming that the shock is strong enough that the precursor is diffusive near the shock. Thus, the relation $J_\mathrm{R}(f_\mathrm{s})/2 = J_u(f_\mathrm{s})$ determines f_s.

Fig. 7 shows the profiles of density and RT, for $Q = 10^6$ and other parameters as indicated. Here, the downstream optical depth is $-\kappa z$, where $z = 0$ at the density jump, while the upstream optical depth is $\overline{\chi} z$, and $\kappa_\mathrm{p} f_\mathrm{E}/\overline{\chi} = 1/3$. Note that the scale of the cooling layer is roughly six orders of magnitude smaller than the scale of the precursor. At this large a value of Q, the transmissive region in the precursor, although present, is not evident in the plots.

VII. Discussion

It was emphasized above that the three-layer model ignores the adaptation zones. Having seen the nature of the solutions, one can consider the qualitative implications of this approximation. In the downstream region, most of the cooling must occur in a small fraction of an optical depth for reasons discussed above. However, detailed radiation transport calculations [35] show that the radiation flux does not decrease all the way to zero at the cooling layer boundary but rather approaches zero slowly as the optical depth from the cooling layer increases. Correspondingly, from (8), the density and temperature also only slowly reach their final values. This will have the effect of creating a long small tail on the heated region in Figs. 4 and 7. The present type of calculation could be improved to capture this behavior by iterating the profile of J_R in the downstream region.

Given the large extent of the precursor, the upstream adaptation zone is comparatively quite small. One can see its qualitative effects as follows. In the diffusive zone, the precursor profile will evolve with a gradual increase in temperature and density along the profile found by the model discussed above. This will continue until the hotter upstream matter begins to affect J_R and F_R as one approaches the density jump. Then, J_R, F_R, η, and T will increase as one moves through the upstream adaptation zone to the density jump. The magnitude of these increases will not be large. The upstream temperature at the shock, for example, is limited from above by (11) and from below because the energy balance still implies that $f_\mathrm{s} = T_\mathrm{ps}/T_\mathrm{f}$ must approach 1 as the shock strength increases.

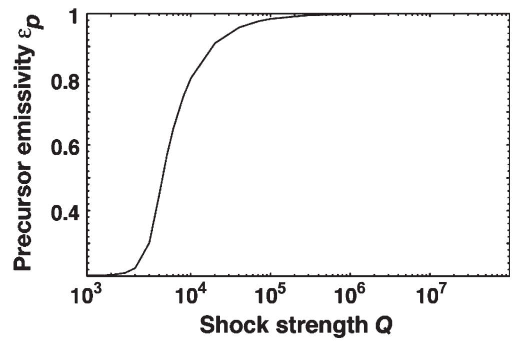

Fig. 8. Precursor emissivity becomes large as Q exceeds 10^4 and asymptotically approaches 1 for large Q.

Given a solution for the precursor profile, one can proceed to find the precursor emissivity ε_p, which is the ratio of the downstream radiation flux at the density jump to σT_ps^4. Fig. 8 shows the results. The precursor emissivity is near unity for strong-enough shocks but falls rapidly as Q drops below 10^4.

VIII. Conclusion

The work presented above provides a complete conceptual description of planar OTR shocks, under conditions in which the radiation transport can be well characterized using spectrally averaged opacities. The key parameter is a measure of the shock strength, labeled Q here, proportional to $u_\mathrm{s}^5/\rho_\mathrm{o}$. At approximately the shock strength where the equilibrium thermal radiation flux from the immediate postshock (and postelectron-ion-equilibration) state exceeds the incoming mechanical energy flux, a diffusive radiative precursor develops upstream of the viscous density jump. The length of this precursor (in optical depth units) increases in rough proportion to Q. The energy carried upstream by this radiation flux returns back across the density jump as a combination of internal energy and radiation. The conversion of some of the upstream radiation to internal energy in the precursor has the ultimate implication that the temperature in the precursor can approach the final downstream temperature only asymptotically, in the limit that the increment of internal energy becomes comparatively negligible. Downstream of the density jump, a cooling layer forms within which the temperature is driven down to nearly its final steady value, with the corresponding increase in density required by the conservation of mass and momentum. The length of this cooling layer is inversely proportional to Q. The fluid dynamics in the above description is exact. The treatment of radiation is approximate but is qualitatively reasonable in the strong-shock limit that the optical depth of the cooling layer is negligible and that the emissivity of the precursor is near unity.

Further work with semianalytic theory could attempt to progress beyond the limitations of the present calculation. In particular, one might develop methods to characterize the spatial evolution of the Eddington factor, with or without allowing for variations in the opacities with the parameters. One might, for example, hope to follow the evolution of the precursor into the diffusive regime from both directions and to find conditions under which the structure was self-consistent. Initial attempts in this direction by the present author have proven numerically challenging.

The interesting experimental case would be the transition into the strong-shock regime. One could hope to observe the development and structure of a diffusive precursor, in particular by measuring the temperature profile. This might prove difficult given the rapid increase of precursor length with shock velocity, but one might make some progress using systems that have cooled below an initial higher temperature, as in the experiments [9] of Hansen *et al.*, thus increasing the overall optical depth. One also might hope to observe the structure of the cooling layer if experiments can be devised to make it large enough. More difficult would be the problem of observing the initial structure in the precursor near the density jump, where the radiation rapidly evolves from a pancaked angular distribution to an isotropic one.

Acknowledgment

The author would like to thank A. Reighard, J. Castor, D. Ryutov, J. Edwards, and S. Bouquet for the useful discussions of this topic.

References

[1] L. Boireau, C. Clique, and S. Bouquet, *Simulations and Experiments on Radiative Shocks, Inertial Fusion Science and Applications*. Monterey, CA: American Nuclear Society, 2003.
[2] S. Bouquet and C. Stehlé, M. Koenig *et al.*, "Observations of laser driven supercritical radiative shock precursors," *Phys. Rev. Lett.*, vol. 92, no. 22, pp. 225 001.1–225 001.4, Jun. 2004.
[3] J. C. Bozier and G. Thiell, J. P. Le-Breton *et al.*, "Experimental observation of the radiative wave generated in xenon by a laser-driven supercritical shock," *Phys. Rev. Lett.*, vol. 57, no. 11, pp. 1304–1307, Sep. 1986.
[4] A. D. Edens and T. Ditmire, J. F. Hansen *et al.*, "Study of high Mach number laser driven blast waves," *Phys. Plasmas*, vol. 11, no. 11, pp. 4968–4972, Nov. 2004.
[5] P. A. Keiter and R. P. Drake, T. S. Perry *et al.*, "Observation of a hydrodynamically-driven, radiative-precursor shock," *Phys. Rev. Lett.*, vol. 89, no. 16, pp. 165 003.1–165 003.4, Sep. 2002.
[6] M. Koenig and A. Benuzzi-Mounaix, N. Grandjouan *et al.*, "Radiative shock experiments using high power laser," in *Proc. Shock Compress. Condens. Matter*, 2001, vol. 620, pp. 1367–1370.
[7] A. B. Reighard and R. P. Drake, K. K. Danneberg *et al.*, *Collapsing Radiative Shocks in Xenon Gas on the Omega Laser, Inertial Fusion and Science Applications*. Monterey, CA: American Nuclear Society, 2003.
[8] ——, "Collapsing radiative shocks in xenon on the Omega laser," *Phys. Plasmas*, vol. 13, no. 8, p. 082 901, Aug. 2006.
[9] J. F. Hansen and M. J. Edwards, D. H. Froula *et al.*, "Laboratory observation of secondary shock formation ahead of a strongly radiative blast wave," *Phys. Plasmas*, vol. 13, no. 2, p. 022 105, Feb. 2006.
[10] Y. A. Fadeyev and D. Gillet, "The structure of radiative shock waves," *Astron. Astrophys.*, vol. 333, no. 2, pp. 687–701, May 1998.
[11] S. K. Chakrabarti and L. G. Titarchuk, "Spectral properties of accretion disks around galactic and extragalactic black holes," *Astrophys. J*, vol. 455, no. 2, pp. 623–639, Dec. 1995.
[12] A. V. Farnsworth and J. H. Clarke, "Radiatively and collisionally structured shock waves exhibiting large emission-convection ratio," *Phys. Fluids*, vol. 14, no. 7, pp. 1352–1360, Jul. 1971.
[13] R. Sivron, D. Caditz, and S. Tsuruta, "Effects of shocks on emission from central engines of active galactic nuclei.1," *Astrophys. J.*, vol. 469, no. 2, p. 542, 1996.
[14] D. Mihalas and B. Weibel-Mihalas, *Foundations of Radiation Hydrodynamics*, Dover (1999) ed. Oxford, U.K.: Oxford Univ. Press, 1984.
[15] S. Bouquet, R. Teyssier, and J. P. Chieze, "Analytical study and structure of a stationary radiative shock," *Astrophys. J. Suppl.*, vol. 127, no. 2, pp. 245–252, Apr. 2000.
[16] V. A. Prokof'ev, "Radiative shocks," *Uch. Zap. Mos. Gos. Univ. Mekh.*, vol. 172, no. 1, p. 79, 1952.
[17] I. P. Raizer, "On the structure of the front of strong shock waves in gases," *Soviet Phys. JETP*, vol. 5, no. 6, pp. 1242–1248, Dec. 1957.
[18] I. B. Zel'dovich, "Shock waves of large amplitude in air," *Soviet Phys. JETP*, vol. 5, no. 5, pp. 919–927, 1957.
[19] J. F. Clarke, "Radiation-resisted shock waves," *Phys. Fluids*, vol. 5, no. 11, pp. 1347–1361, Nov. 1962.
[20] M. Mitchner and M. Vinokur, "Radiation smoothing of shocks with and without a magnetic field," *Phys. Fluids*, vol. 6, no. 12, pp. 1682–1692, Dec. 1963.
[21] S. C. Traugott, "Shock structure in a radiating, heat conducting and viscous gas," *Phys. Fluids*, vol. 8, no. 5, pp. 834–849, May 1965.
[22] A. J. Skalafuris, "Radiative shock structure—Theory and observations," *J. Quant. Spectrosc. Radiat. Transf.*, vol. 8, no. 1, pp. 515–530, Jan. 1968.
[23] Y. B. Zel'dovich and Y. P. Razier, *Physics of Shock Waves and High-Temperature Hydrodynamic Phenomena*, Dover (2002) ed. New York: Academic, 1966.
[24] J. Castor, *Radiation Hydrodynamics*. Cambridge, U.K.: Cambridge Univ. Press, 2004.
[25] C. Michaut and C. Stehle, S. Leygnac *et al.*, "Jump conditions in hypersonic shocks," *Eur. Phys. J. D*, vol. 28, no. 3, pp. 381–392, Mar. 2004.
[26] M. A. Heaslet and B. S. Baldwin, "Predictions of the structure of radiation-resisted shock waves," *Phys. Fluids*, vol. 6, no. 6, pp. 781–791, Jun. 1963.
[27] R. I. Klein, R. F. Stein, and W. Kalkofen, "Radiative shock dynamics. I. The Lyman continuum," *Astrophys. J.*, vol. 205, no. 2, pp. 499–519, Apr. 1976.
[28] ——, "Radiative shock dynamics. II. Hydrogen continua," *Astrophys. J.*, vol. 220, no. 2, pp. 1024–1040, Mar. 1978.
[29] L. Ensman and A. Burrows, "Shock breakout in SN 1987A," *Astrophys. J.*, vol. 393, no. 2, pp. 742–755, Jul. 1992.
[30] M. W. Sincell, M. Gehmeyr, and D. Mihalas, "The quasi-stationary structure of radiating shock waves. I. The on-temperature fluid," *Shock Waves*, vol. 9, no. 6, pp. 391–402, Dec. 1999.
[31] D. R. Leibrandt, R. P. Drake, and J. M. Stone, "ZEUS-2D simulations of laser-driven radiative shock experiments," *Astrophys. Space Sci.*, vol. 298, no. 1/2, pp. 273–276, Jul. 2005.
[32] D. R. Leibrandt and R. P. Drake, A. B. Reighard *et al.*, "Validation of the flux-limited diffusion approximation for radiation hydrodynamics," *Astrophys. J.*, vol. 626, no. 1, pp. 616–625, Jun. 2005.
[33] R. P. Drake, *High Energy Density Physics: Fundamentals, Inertial Fusion and Experimental Astrophysics*. New York: Springer-Verlag, 2006.
[34] J. M. Laming and J. C. Raymond, B. M. McLaughlin *et al.*, "Electron-ion equilibration in nonradiative shocks associated with SN 1006," *Astrophys. J.*, vol. 472, no. 1, pp. 267–274, Nov. 1996.
[35] R. P. Drake, "Theory of radiative shocks in optically thick media," *Phys. Plasmas*, to be published.

R. Paul Drake received the Ph.D. degree from The John Hopkins University, Baltimore, MD, in 1979.

He was an Associate Professor at the University of California, Davis, from 1989 to 1991 and a Full Professor from 1991 to 1993. After his Ph.D. thesis research in plasma spectroscopy, he studied magnetic confinement and plasma-surface interactions for the magnetic fusion program at Livermore until 1982. He then joined the laser fusion program there, where he conducted research in laser-plasma interactions, including experiments, optical diagnostics, and theory, while leading various projects including the activation of target experiments on the Nova laser facility during 1984 and 1985. He served as the Group Leader for Plasma Physics from 1985 to 1989. He moved to Michigan in 1996, following service as the Director of the Plasma Physics Research Institute, Lawrence Livermore National Laboratory, from 1989 to 1996. He is currently a member of the Department of Atmospheric, Oceanic, and Space Sciences and the Applied Physics Program, University of Michigan, Ann Arbor, where he leads a group whose research is in experimental astrophysics, i.e., the use of laboratory tools to study dynamic processes and properties of matter that are important for astrophysics. He has authored more than 170 papers describing scientific results.

Dr. Drake is a Fellow of the American Physical Society.